Key Engineering Materials Vols 622-623 (2014) pp 525-531 *Online: 2014-09-26*

doi:10.4028/www.scientific.net/KEM.622-623.525

Numerical Analysis of Welding Phenomena in High-Frequency Electric Resistance Welding

OKABE Takatoshi[1, a *], TOYODA Shunsuke[1, b], GOTO Sota[1, c],
KATO Yasushi[1, d], YASUDA Koichi[2, e], and NAKATA Kazuhiro[3, f]

[1]Steel Research Laboratory, JFE Steel Corp., 1-1, Kawasaki-cho, Handa, Aichi, Japan

[2]Steel Research Laboratory, JFE Steel Corp., 1-1, Kawasaki-cho, Chuo, Chiba, Japan

[3]Joining and Welding Research Institute, Osaka University, 11-1, Mihogaoka, Ibaraki, Osaka, Japan

[a]ta-okabe@jfe-steel.co.jp, [b]s-toyoda@jfe-steel.co.jp, [c]s-goto@jfe-steel.co.jp

[d]y-kato@jfe-steel.co.jp, [e]ko-yasuda@jfe-steel.co.jp, [f]nakata@jwri.osaka-u.ac.jp

Keywords: High-frequency electric resistance welding, Welding phenomenon, Finite element analysis, Numerical analysis.

Abstract. High-frequency electric resistance welded pipes are used for high-grade line pipes. To address the significant need for weld seam reliability, it is important to clarify the associated welding phenomena. In this study, a numerical analysis model is developed to clarify the behaviours of the molten steel and oxide in HFW pipes. The temperature distribution of the HFW is calculated using electromagnetic and heat conductive finite element analysis methods. The molten metal and oxide flows are analysed by modelling heat conductive and plastic flows. The movement behaviour of the oxides in the molten steel is successfully analysed with this technique. The material properties as a function of the temperature of the steel pipe are calculated using general-purpose simulation software. With pressurisation by the welding rolls, the molten steel moves to the upper part, and the oxide, which exists in the internal parts, rapidly decreases such that almost all of the oxide transitions to the excess metal part. The internal oxide content rate after pressurisation at 0.08 m/s is less than 0.01. To decrease the oxide content, the pressurisation rate must increase such that the molten steel and an oxide pressurised at high temperatures transition to the excess metal part.

1. Introduction

High-frequency electric resistance welded (HFW) steel pipes have many excellent properties, such as clean skin surfaces and accurate shape dimensions, both of which allow for increased productivity. The manufacturing processes and quality control technologies used for HFW steel pipes have significantly advanced many research and technological developments. As a result, HFW steel pipes are used in a wide range of applications as line pipes as well as in machine structures.

However, the quality of the weld seams on HFW steel pipes makes it necessary to assess the weld seam reliability. Metal oxides are formed on the surface of the molten metal in the welding. It is important to squeeze out the metal oxides and molten metal by the pressurisation from welding rolls. Many studies have investigated high-frequency welding phenomena and the mechanisms of weld formation [1-5]. Research has also been conducted to directly observe these phenomena and perform numerical analyses [6,7]. In this study, we develop a numerical analysis system to clarify the movement of oxides in molten metal used for HFW steel pipes. The influence of the welding conditions on the behaviour of the molten steel and oxide are investigated using this newly developed analysis system.

2. Analysis System

Fig. 1 presents an overview of the calculation. The temperature distribution can be calculated using electromagnetic and heat conductive finite element analysis methods [7]. We use the general-purpose ANSYS ver.13 solver made by ANSYS, Inc.

Another two-dimensional model of a cross section of the V-convergence point is also produced. The flow behaviour of the molten steel and oxide after pressurisation by the welding rolls is analysed. Using the temperature distribution of the V-convergence point calculated in the above method as the initial value, the heat conductive and plastic flow analyses are executed. Fig. 2 presents the meshes used for the heat conductive and plastic flow analyses. It is assumed that an oxide film of uniform thickness exists on the surface of the molten steel. Fig. 3 presents the meshes used for the oxide film, which expands along the horizontal axis. The minimum mesh length in the circumferential direction is 0.02 mm. The number of meshes in the analysis model is estimated to be 25,000. The analysis model is divided into four parts according to the symmetry of the pipe. We use the general-purpose FLUENT 14 solver made by ANSYS, Inc. The unsteady thermal hydraulics analytical method considering two-phase flow and a free surface is used. This method requires approximately one week for a single analysis using a personal computer with an Intel Xeon E5-2687W CPU 3.1 GHz processor.

Tables 1–3 present the material properties used in the analyses. The density, specific heat, thermal conductivity, viscosity, relative permeability, and electric resistance of the low-carbon, low-alloy steel are analysed as a function of temperature. These data are calculated using the JMatPro ver.7 general-purpose software made by Sente Software Ltd. The material properties of FeO are used for the oxide. Table 4 provides the specific heat of the oxide. Constant values are assumed for the density of the oxide (4,500 kg/m^3), the thermal conductivity (5 W/(m·K)), and the viscosity (0.05 kg/(m·s)). Table 5 presents the numerical analysis conditions. The influence of the pressurisation rate from the welding rolls and the thickness of the oxide film on the behaviour of the molten steel and oxide are investigated.

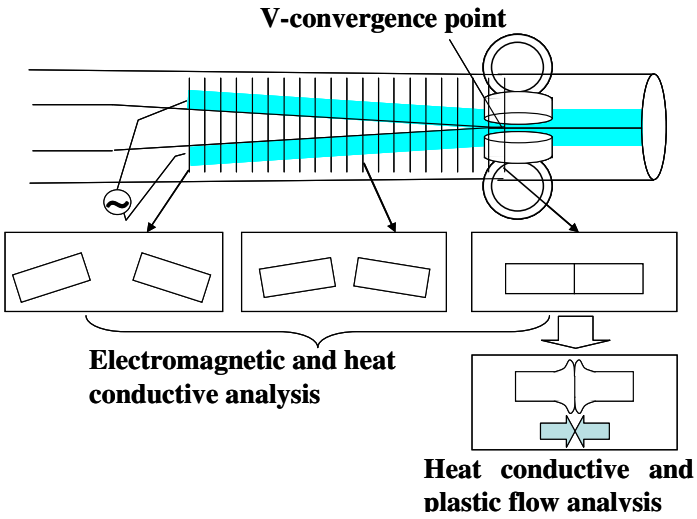

Fig. 1 Overview of the numerical analysis system.

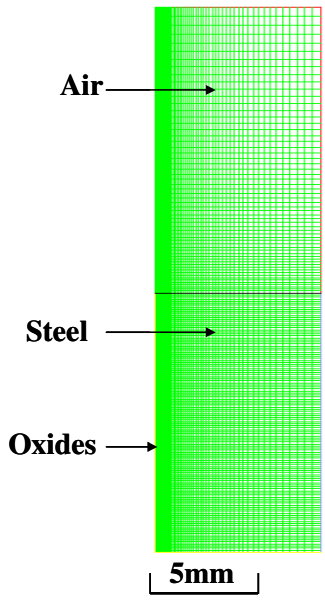

Fig. 2 Mesh used in the heat conductive and plastic flow analysis approach.

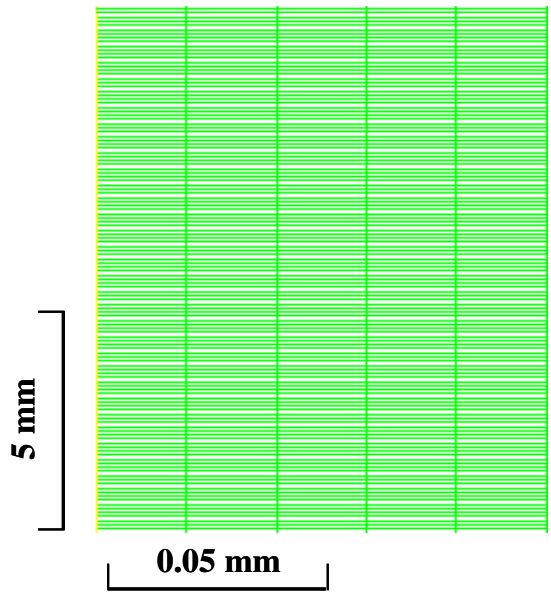

Fig. 3 Oxide mesh used in the heat conductive and plastic flow analysis approach.

Table 1 Material properties of the pipe.

Temperature [℃]	Density [kg/m^3]	Specific heat [J/(kg·K)]	Thermal conductivity [W/(m·K)]	Viscosity [kg/(m·s)]
25	7843	451	52.8	-
115	7818	501	50.8	-
225	7791	528	46.1	-
490	7702	744	37.7	-
515	7696	795	36.6	-
600	7685	1119	32.1	-
660	7704	1313	27.8	-
725	7708	687	25.9	-
745	7700	620	26.0	-
1435	7319	693	34.3	6.48
1440	7315	1636	34.3	6.00
1465	7279	1267	34.5	2.93
1470	7274	733	34.6	2.62
1495	7262	737	34.9	2.10
1500	7257	2292	35.0	1.95
1510	7225	4738	35.0	1.14
1520	7136	15128	34.6	0.18
1525	7016	35110	33.9	0.01
1530	6988	822	33.8	0.01
1595	6935	827	35.0	0.01

Table 2 Relative permeability of the pipe.

Temperature [℃]	Relative permeability
25	271
143	282
252	299
366	326
478	364
592	415
688	466
699	471
703	455
705	445
731	450
733	450
738	449
743	446
755	415
760	358
762	299
765	1
1595	1

Table 3 Electrical resistance of the pipe.

Temperature [℃]	Electric resistance [x10^7 Ω·m]
25	1.8
140	2.7
260	3.8
370	5.0
485	6.5
590	8.6
660	10.9
705	12.3
790	13.1
820	13.3
930	13.9
1040	14.5
1150	15.0
1265	15.6
1370	16.0
1500	16.5
1535	17.4
1595	17.4

Table 4 Specific heat of the oxide.

Temperature [℃]	Specific heat [J/(kg·K)]
27	671
527	766
700	789
927	816
1200	849
1250	855
1320	863
1350	8054
1380	8141
1410	950
1500	950
1727	950

Table 5 Numerical analysis conditions.

Wall thickness	25 mm
Outer diameter	610 mm
Welding speed	0.2 m/s
V-convergence angle	5°
Welding frequency	300 kHz
Distance between electrode and V-convergence point	300 mm
Pressurisation amount	5 mm

3. Simulation Results and Discussion

Fig. 4 presents the isothermal diagram of the V-convergence point calculated by the electromagnetic and heat conductive finite element analysis. Using this temperature distribution as an initial value, a 0.1-mm-thick oxide film is assigned to the surface of the molten metal, and the heat conductive and plastic flow analyses are executed. The pressurisation rate is 0.02 m/s.

Fig. 5 presents the phase distribution during the pressurisation from the welding rolls. The entire upper portion of the weld begins to rise immediately after pressurisation begins. Furthermore, the molten steel moves to the upper part upon pressurisation. The height of the molten steel of the welding edge after pressurisation is complete increases by approximately 70% compared with the initial state. The oxide moves the welded surface to the upper part immediately after pressurisation. After 0.06 s, most oxides move to the excess metal part and upper part, agitating the inside of the excess metal over time. After 0.25 s, the pressurisation is complete, and the oxide distributes into the upper part of the reinforcement of the weld.

Fig. 6 presents the relationship between the time and oxide content ratio for initial oxide content in positions other than the reinforcement weld (hereafter described as the internal part) at pressurisation rates ranging from 0.02 to 0.08. Immediately after the pressurisation begins, the oxide content decreases rapidly and becomes constant for every pressurising condition. The oxide content after pressurisation is 0.05 or less for all pressurisation speeds. The oxide content after pressurisation decreases with increasing pressurisation rate. The oxide content after the pressurisation at 0.08 m/s is less than 0.01.

Fig. 7 presents the phase distribution diagrams after 0.02 s for pressurisation rates of 0.02 and 0.08 m/s. At 0.02 m/s, the weld zone rises smoothly, and the oxide moves to the internal part. In contrast, at 0.08 m/s, the weld zone rises rapidly, and almost all of the oxide moves to the excess metal part. Because 0.08 m/s represents a high degree of pressurisation compared to 0.02 m/s at high temperatures, it is presumed that a large portion of the molten steel moves to the excess metal part. It is also presumed that the oxide moves to the excess metal part with the movement of the molten steel because the oxide is present on the surface of or inside the molten steel. In contrast, because 0.02 m/s is less pressurised, the molten steel exists in the internal part. As a result, it is presumed that the oxide also exists inside the molten steel. As the weld zone cools rapidly, the molten steel solidifies. When the molten steel solidifies in the internal part, the oxide also is present in the internal part. If the molten steel solidifies, even if it is pressurised, it will move only slightly. The oxide will also move only slightly. Because the molten steel may solidify over time, it is presumed that the oxide reaches an

almost constant value, as shown in Fig. 6. When the pressurisation rate is slow, the oxide in the internal parts increases because the molten steel is solidified without moving completely to the excess metal part. As mentioned above, to decrease the oxide content in the internal parts, the pressurisation rate must increase such that the molten steel and oxide are pressurised rapidly at a high temperature and move to the excess metal part. From the view point of the weld seam reliability, it is presumed that the increase of the pressurisation rate is effective for the prevention of the welding defect.

Fig. 8 presents the effect of the initial oxide film thickness on the oxide content in the internal part after pressurisation. The oxide content decreases as the initial oxide film thickness decreases. The initial oxide film thickness must be decreased to decrease the oxide content in the internal parts. The thickness of the oxide generated in the heating process is several micrometres. Therefore, the oxide content rate in the internal parts becomes 0.01 or less.

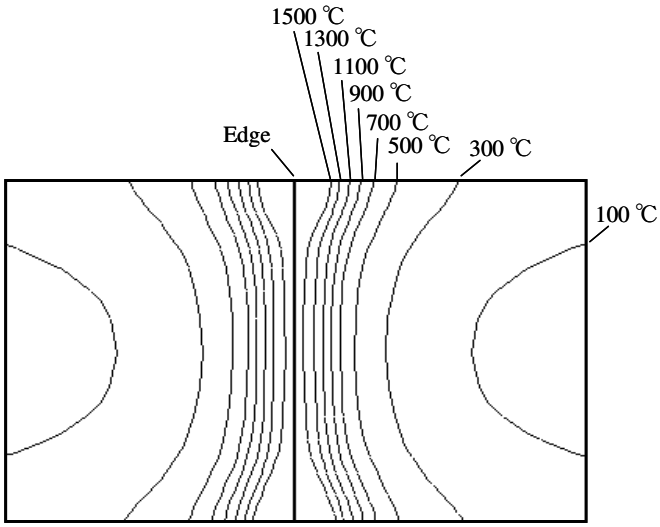

Fig. 4 Isothermal diagram of the V-convergence point.

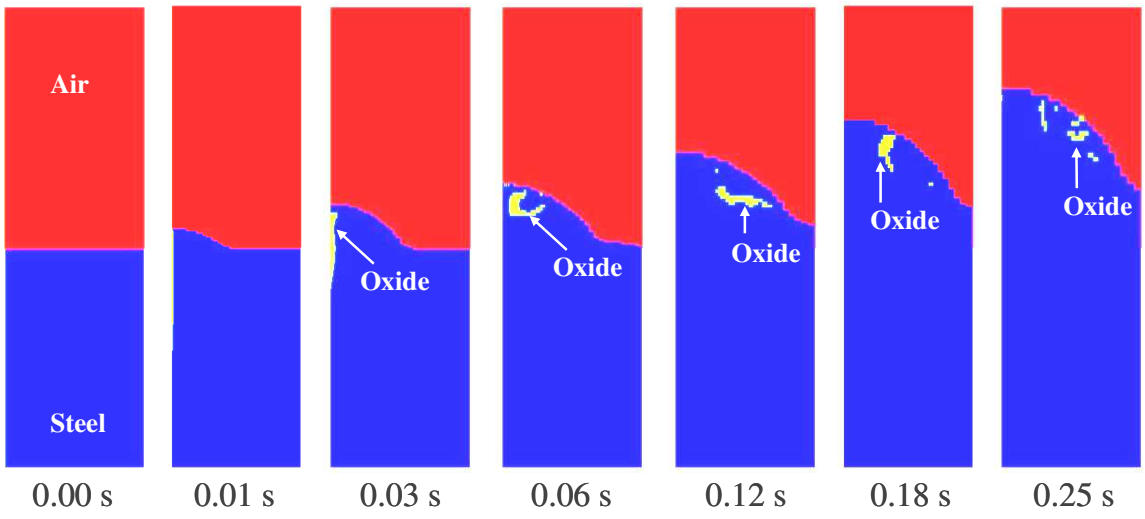

Fig. 5 Phase distribution during the pressurisation by the welding rolls.

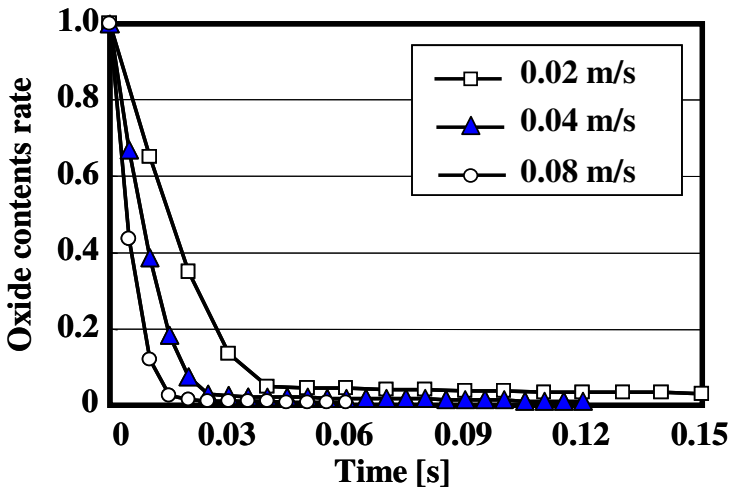

Fig. 6 Oxide content in the removed portion of the oxide in the excess metal portion over time. The initial oxide content is 1.

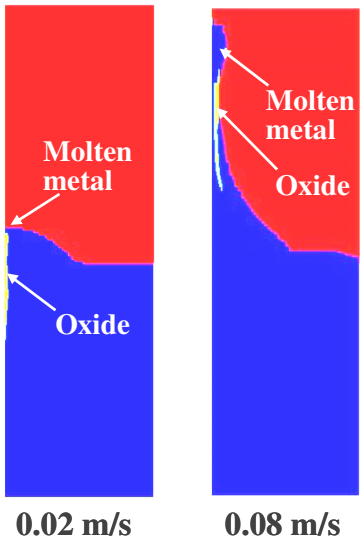

Fig. 7 Phase distribution after 0.02 s.

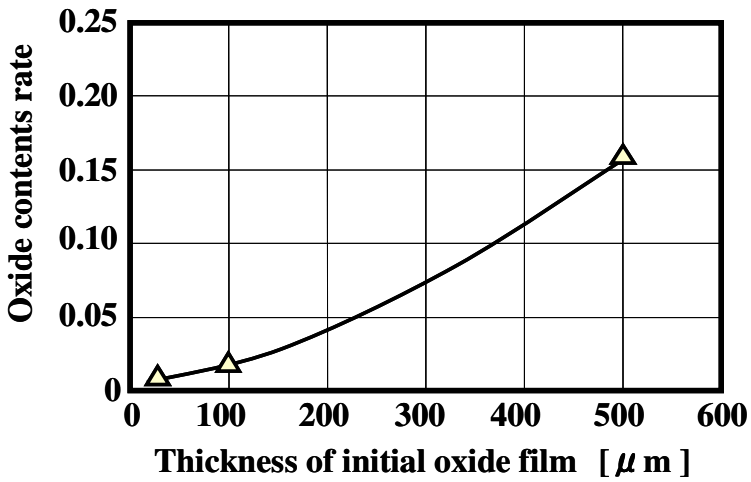

Fig. 8 Relationship between the thickness of the initial oxide film and the contents of oxide present in the removed portion of the oxide in the excess metal portion. The initial oxide content at a thickness of 100 μm is 1.

4. Conclusion

A high-frequency welding analysis system combining electromagnetic, heat conductive, and plastic flow analyses was developed. The movement behaviour of oxides in the molten metal used for HFW steel pipes was analysed.

(1) The temperature distribution of the V-convergence point was calculated by the electromagnetic and heat conductive analysis method. Using these results, the heat conductive and plastic flow analyses were executed. The movement behaviour of metal oxides in the molten metal were successfully analysed with this technique.

(2) The molten steel moved to the upper part with pressurisation by welding rolls. Most oxides moved to the excess metal part and the upper part, agitating the inside of the excess metal part over time. After pressurisation was complete, the oxide distributed in the upper part of the reinforcement of the weld.

(3) Immediately after pressurisation, the oxide content decreased rapidly and became almost constant for every pressurising condition. The oxide content after pressurisation was 0.05 or less for all pressurisation speeds.
(4) The oxide content after pressurisation decreased with an increasing pressurisation rate. When the pressurisation rate was slow, the oxide content in the internal parts increased because the molten steel was solidified without moving completely to the excess metal part.
(5) To decrease the oxide content in the internal parts, the pressurisation rate had to be increased such that the molten steel and oxide rapidly pressurised at a high temperature and moved to the excess metal part. From the view point of the weld seam reliability, it is presumed that the increase of the pressurisation rate is effective for the prevention of the welding defect.
(6) The oxide content decreased with decreases in the initial oxide film thickness. It was necessary to decrease the initial oxide film thickness to decrease the oxide content.

References

[1] H. Haga, K. Aoki and T. Sato: Welding Phenomena and Welding Mechanisms in High Frequency Electric Resistance Welding-1st Report, Welding J., July (1980), 208-212.

[2] H. Haga, K. Aoki and T. Sato: The Mechanisms of Formation of Weld Defects in High-Frequency Electric Resistance Welding, Welding J., June (1981), 104-109.

[3] S. Suzuki and T. Takamura: The Formation Mechanism of White Line in Welded Joints of ERW Steel Pipes: Tetsu-to-Hagane, 70 (1984), 1467-1373. (in Japanese)

[4] T. Toyoda, T. Miyakawa, K. Ueyama and T. Morisue: Development of Welding Heat Pattern Model at ERW 16inch mill, Current Advances in Materials and Processes, 3 (1990)2, 542-543. (in Japanese)

[5] N. Okada, H. Sakamoto, T. Matsuo and K. Takatani: Numerical Analysis Model of Electric Resistance Welding Pipe, Tetsu-to-Hagane, 98 (2012), 368-377. (in Japanese)

[6] T. Okabe, K. Kenmochi and K. Sakata: Electro Magnetic and Heat Conductive FE Analysis on High Frequency Tube Welding Process, Tetsu-to-Hagane, 93 (2007), 373-378. (in Japanese)

[7] T. Okabe, M. Aratani, Y. Yokoyama, S. Toyoda, H. Kimura, M. Egi and A. Kawanishi: Finite Element Analysis of the Electric Resistance Welding Phenomenon, Steel Research International Special Edition: 10th International Conference on Technology of Plasticity, ICTP2011, (2011), 662-666.

Metal Forming 2014
10.4028/www.scientific.net/KEM.622-623

Numerical Analysis of Welding Phenomena in High-Frequency Electric Resistance Welding
10.4028/www.scientific.net/KEM.622-623.525

DOI References
[5] N. Okada, H. Sakamoto, T. Matsuo and K. Takatani: Numerical Analysis Model of Electric Resistance Welding Pipe, Tetsu-to-Hagane, 98 (2012), 368-377. (in Japanese).
http://dx.doi.org/10.2355/tetsutohagane.98.368
[6] T. Okabe, K. Kenmochi and K. Sakata: Electro Magnetic and Heat Conductive FE Analysis on High Frequency Tube Welding Process, Tetsu-to-Hagane, 93 (2007), 373-378. (in Japanese).
http://dx.doi.org/10.2355/tetsutohagane.93.373